ISBN: 978-628-96613-1-6. ISSN: 2414-6390. Digital Object Identifier: https://dx.doi.org/10.18687/LACCEI2025.1.1.1078

Prediction of electrical energy generation from photovoltaic plants with NARX neural network

Elmer Arellanos-Tafur[1,2,5], Felix Rojas-Arquiñego[3] and Marcelo Damas-Niño[4]
[1] Universidad Tecnológica del Perú, Peru, c19083@utp.edu.pe
[2] Universidad de Ingenieria y Tecnologia - UTEC, Peru, earellanos@utec.edu.pe
[3] Universidad Señor de Sipan, Peru, felixrojas@uss.edu.pe
[4] Universidad Nacional del Callao, Peru, mndamasn@unac.edu.pe
[5] Universidad Continental, Peru, earellanos@continental.edu.pe

***Abstract*—The integration of renewable energy sources into existing power grids presents significant challenges due to their inherent variability. This research investigates the application of Nonlinear Autoregressive Exogenous (NARX) neural networks for accurate prediction of electrical energy generation from photovoltaic plants. Solar energy forecasting is crucial for effective grid management, energy trading, and optimal operation of photovoltaic installations. The study employed a correlational research design to analyze the relationship between NARX neural networks (variable X) and the accuracy of electrical energy generation prediction from photovoltaic plants (variable Y). Using time series data from two operational solar plants—a 112.04 kW installation in La Palma del Condado (Huelva, Spain) and a 75.24 kW facility in Alcalá del Río (Seville, Spain)—the research developed predictive models that incorporated both historical energy production values and solar radiation measurements. The methodology followed a systematic approach including neural network construction, training, validation, and testing phases. Performance evaluation through linear regression analysis revealed remarkably high prediction accuracy, with correlation coefficients (r) of 0.991 and 0.968 for the two case studies, respectively, yielding an average accuracy of 97.9%. The results demonstrate that NARX neural networks provide highly reliable forecasting capabilities for photovoltaic energy generation, which can significantly contribute to reducing operational costs, minimizing the need for backup energy sources, and facilitating the broader integration of solar power into existing electricity grids.**

Keywords: Prediction, photovoltaic energy, NARX, network.

I. Introduction

Currently, the transition to sustainable energy systems has become a global priority due to the increasing impacts of climate change and the need to reduce greenhouse gas emissions. Additionally, environmental protection and energy consumption reduction have garnered significant attention in the 21st century [1]. Energy sources are a crucial material foundation for social development, while reliable electricity supply is a critical support for modern civilization [2]. In this context, renewable energies, with photovoltaic solar energy among the prominent ones, emerge as key solutions to mitigate the negative environmental effects of fossil fuels and promote more sustainable development. Photovoltaic solar energy, in particular, stands out for its ability to directly convert solar radiation into electricity through photovoltaic cells, making it a central technology in the sustainable energy agenda. The U.S. Energy Information Agency predicts that renewable resources will be the fastest-growing source of energy generation, reaching 17% of total energy consumed in the United States by 2035 [3]. Photovoltaic (PV) and wind technologies currently constitute over 60% of global annual net additions to capacity [4], with off-grid PV installations increasingly used in developing countries where the conventional electricity grid cannot reach [5]. Furthermore, electricity generation from mainstream photovoltaic (PV) technologies, dominated by rooftop solar and utility scale solar plants, has established itself as one of the cheapest sources of electricity [6], considerably cheaper than alternative nonrenewable energy sources (coal, gas, and nuclear) [7]. Taking advantage of this, other photovoltaic applications such as building-integrated PV [8]– [9], vehicle-integrated PV [10], and space PV [11]– [12], have also experienced considerable growth in recent years [13], positioning PV technology to become one of the dominant sources of global electricity generation and a key foundation of future energy systems [14]. Despite its advantages, photovoltaic energy generation faces significant challenges due to the inherent variability and intermittency of solar resources. Accurately forecasting energy output at photovoltaic (PV) plants is essential for maximizing operational efficiency and ensuring the stability of electricity supply—particularly in scenarios where the integration of renewable energy sources with conventional power grids must be carefully managed to prevent overloads and maintain consistent delivery. In this context, advanced modeling and forecasting techniques, such as artificial neural networks, have gained relevance for enhancing prediction accuracy. Nonlinear autoregressive neural networks with exogenous inputs (NARX) are especially promising due to their ability to model complex dynamics and leverage both historical and exogenous data to produce accurate forecasts, effectively addressing the challenges posed by solar variability. This study evaluates the predictive accuracy of a NARX neural network applied to electricity generation in PV plants. The analysis offers a comprehensive perspective on the network's

.

effectiveness, providing valuable insights for optimizing resource management and advancing toward a more efficient and sustainable energy system.

II. Theoretical framework

A. Photovoltaic Energy Generation

Photovoltaic technology is among the most relevant renewable energy resources in the contemporary context. Through this technology, the direct conversion of solar radiation into electricity is carried out via photosensitive semiconductor devices. This process presents optimal sustainability characteristics by not generating polluting byproducts during its operational phase. The determining Factors in Photovoltaic Production are:

- Solar Radiation and Seasonal Variability: The availability of the primary solar resource shows significant seasonal variability as a function of the seasonal cycle. During the summer period, the extension of daylight intervals maximizes photovoltaic performance. In contrast, during the winter months, energy generation is reduced due to the decrease in daylight duration.
- Geographic Location: Latitudinal positioning constitutes a critical parameter for determining photovoltaic potential. Regions near the Earth's equator receive solar irradiation of greater intensity and annual homogeneity.
- Atmospheric Conditions: Atmospheric factors such as cloud cover and dust significantly impact photovoltaic performance. Even under partially cloudy sky conditions, generation is maintained, albeit with reduced efficiency.
- Technological Configuration: The typology of photovoltaic cells used, the system architecture, and the orientation of the capturing modules constitute determining technical factors. Solar tracking systems significantly increase energy capture by continuously optimizing the angle of incidence.
- Operating Temperature: High temperatures can paradoxically reduce the efficiency of photovoltaic devices. Most modules experience degradation in their performance when their operating temperature exceeds 25°C, a phenomenon characterized as a "negative temperature coefficient".

B. Neural networks

A key development in artificial intelligence, neural networks represent a computational model inspired by the biological neural architecture. This mathematical model, composed of interconnected units called artificial neurons, serves as an invaluable tool for solving complex and multifaceted problems. In the realm of neural networks, the hierarchical structure of layers is a cardinal element. These layers, classified as input, hidden, and output layers, enable the progressive transformation of raw data into higher-level abstract representations. The activation function, a fundamental component of neural networks, introduces nonlinearity into the model, allowing it to capture intricate relationships between input and output data. In a neural network, the activation function is responsible for converting the weighted sum of each node's inputs into the corresponding activation or output [15]. Many researchers employ different activation functions, such as the binary activation function, linear activation function, exponential linear activation function, Rectified Linear Unit (ReLU), Softmax activation function, and Sigmoid activation function, among others [16]. In the training process, the backpropagation algorithm plays a fundamental role. This algorithm, based on the chain rule of differential calculus, allows for the efficient updating of synaptic weights by calculating the gradient of the error with respect to each weight.

C. NARX model

In recent years, artificial intelligence technology has developed rapidly [17]. NARX model is a nonlinear autoregressive neural network with exogenous inputs. NARX is a recurrent dynamic neural network architecture used to model input-output nonlinear systems. NARX uses the present input, past input and past output to model the nonlinear system dynamic [18]- [19]. Like the NAR network, this network is a type of multilayer perceptron in which after having the data series to be applied we define the lags, the number of hidden layers and the training function. In this network there will be an output variable that depends on several input variables. The equation that defines the NARX model is the following:

$$y(t) = f(y(t-1),y(t-2),...,y(t-ny),u(t-1),u(t-2),...,u(t-nu))$$

where the next value of the dependent output signal y(t) is regulated by previous values of the output signal and previous values of an independent (exogenous) input signal. It is considered that the output of the NARX network can be an estimate of the output of a nonlinear dynamic system that is being attempted to model. The output is returned to the input of the feedforward neural network. This is considered a feedforward backpropagation network with feedback from the output to the input. The architecture is shown in Figure 1 [20].

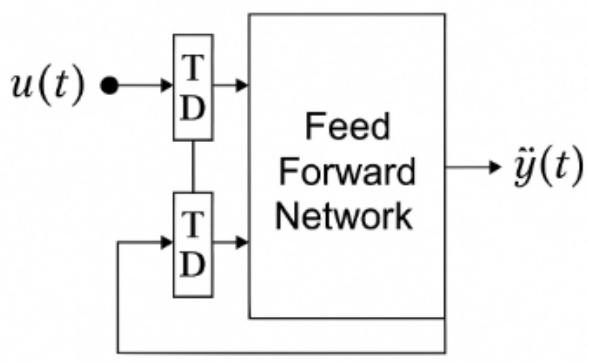

Fig. 1. NARX parallel architecture

Because the actual output is available during network training, a series-parallel architecture can be created in which the

actual output is used in feedback of the estimated output. The architecture is shown in Figure 2.

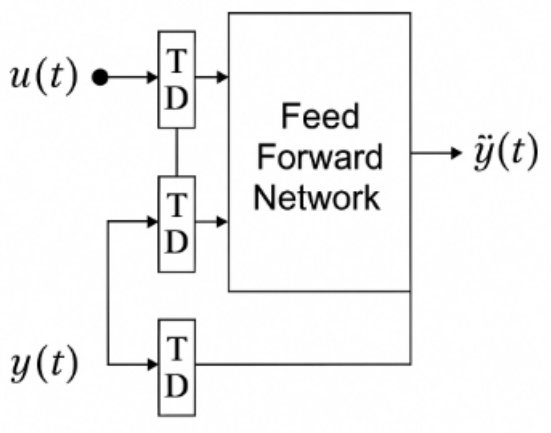

Fig. 2. NARX parallel serial architecture

Figure 3 illustrates in detail the components of the general structure of a NARX neural network and Figure 4 gives us the meanings of the symbols used [21].

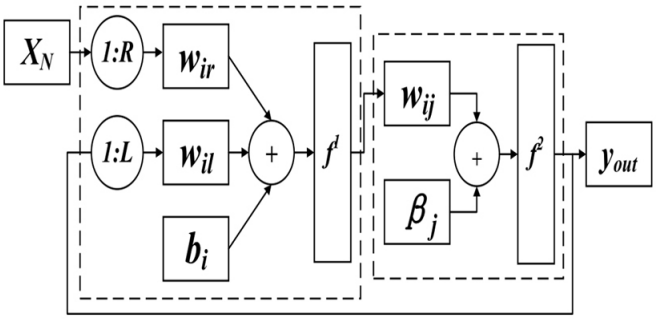

Fig. 3. Structure of NARX

symbol	meaning
f	The activation function of hidden layer or output layer.
R	The time-delay order of input.
L	The time-delay order of output.
w_{ir}	The weight between the ith node of hidden layer and the rth time-delay node of input.
$x_{(t-r)}$	The current and delay values of input.
w_{il}	The weight between the ith node of hidden layer and the lth time-delay node of output.
$y_{(t-l)}$	The current and delay values of output.
b_i	The bias of the ith node of hidden layer.
w_{ij}	The weight between the ith node of hidden layer and the jth node of output layer.
β_j	The bias of the jth node of output layer.

Fig. 4. Meanings for symbols of NARX

A NARX neural network is the most widely used type of neural network in nonlinear dynamic systems and is suitable for time series prediction. Consequently, NARX neural networks have been applied to solve nonlinear sequence prediction problems in many fields. The memory effect of a NARX neural network on historical data enhances its processing ability for dynamic data and improves its prediction performance for complex series. Furthermore, NARX neural networks have a stronger mirroring capability for nonlinear fitting than other neural networks and are more suitable for the analysis and prediction of time series data such as tide level data [22]-[23].

D. Time series

A time series comprises a collection of values for a particular variable, arranged according to the moments at which they were recorded, typically at regular time intervals. Time series analysis involves addressing problems where observations are logged at specific time intervals and where there are correlations between consecutive observations. Its applications extend across nearly every scientific field. The primary objective of time series analysis is to discern the underlying structure of the phenomena generating the observations. By comprehending the mechanisms of a time series, we can formulate mathematical models that aim to describe the data, facilitating tasks such as prediction, monitoring, and control. It is presumed that the dataset of the time series under examination exhibits a systematic pattern. Common patterns include trends, which are usually linear or quadratic, and seasonality, a trend that systematically recurs over time.

E. The Levenberg-Marquardt algorithm

An amalgam of the Gauss-Newton and gradient descent methods, the Levenberg-Marquardt algorithm stands out as a leading technique for minimizing nonlinear functions, especially in curve fitting. Its strength lies in blending the robustness of gradient descent with the speed of Gauss-Newton, making it both versatile and reliable. A key advantage is its rapid convergence near the optimal solution, often surpassing other methods in computational efficiency. Nonetheless, its performance depends heavily on the choice of damping parameter and initial conditions. In complex, multivariate landscapes, the algorithm may struggle with local minima, highlighting the value of heuristic enhancements. Its impact goes beyond theory, finding broad applications from engineering model calibration to neural network training. Its capacity to manage large datasets and adapt across domains makes it a vital tool for data scientists and engineers.

III. Methodology

A correlational design was selected for this investigation, as the current study aimed to ascertain the extent of the relationship between two or more variables of interest within the same sample of subjects, or the extent of the relationship between observed phenomena or events. See the implemented design in Figure 5.

The correlational design facilitated the description of the relationship between two variables: X = Artificial Neural

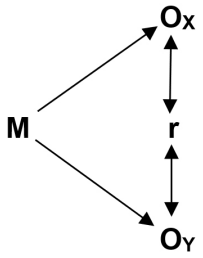

Fig. 5. Correlational design

Networks and Y = Prediction of Energy Generation from Photovoltaic Panels.

In this context, "M" represents the sample in which the study was conducted, while the subscripts "x, y" in each "O" denote the observations obtained for each of the two distinct variables (x, y). Lastly, "r" refers to the relationship between the variables under investigation.

IV. Implementation and Results

For the implementation of the research the data were taken from two photovoltaic solar plants [24]: the 112.04 kW solar plant in La Palma del Condado, Province of Huelva, Spain for case 1 and the 75.24 kW solar plant in Alcalá del Río, Province of Seville, Spain for case 2, as illustrated in the Table I.

TABLE I
Study population

Solar plants	Characteristics	Location
Solar plant - 112.04 kW	Consisting of 520 polycrystalline photovoltaic panels with fixed structure and single-axis tracking	La Palma del Condado, Province of Huelva, Spain
Solar plant - 75.24 kW	Consisting of 342 monocrystalline photovoltaic panels with dual-axis tracking	Alcalá del Río, Province of Seville, Spain

Linear regression analysis of the network outputs and the corresponding objectives was used as a statistical test. Linear regression returns three parameters. The first two: m and b, correspond to the slope and the y-intercept. The best linear regression identically relates objectives to network outputs. If there were a perfect fit (outputs exactly equal to the targets), the slope would be 1, and the y-intercept would be 0. The third variable returned by the regression is the correlation coefficient "r" between the outputs and the targets. Which is a measure of how much of the primary solar resource is explained by the objectives. If this number is equal to 1, then there is a perfect correlation between the objectives and the outputs.

A. Implemented Algorithm

The flowchart of the implemented algorithm is shown in Figure 6. The details of the implemented steps are as follows:

Collect data:

- Time series of energy production from solar plants
- Corresponding solar radiation measurements

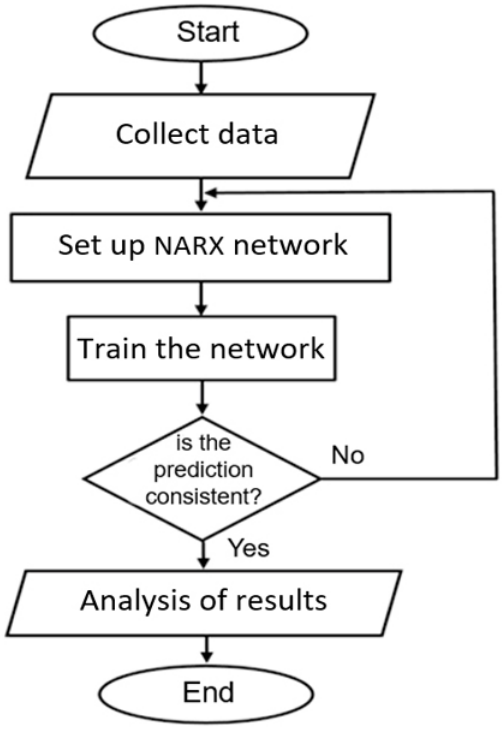

Fig. 6. Steps of the implemented algorithm

Set up NARX network:

- Configure one neuron in hidden layer
- Establish 1-2 time delays for feedback
- Define two inputs: external data and feedback

Train the network:

- Apply Levenberg-Marquardt algorithm
- Split data into training, validation, and test sets
- Monitor Mean Squared Error (MSE)
- Stop when validation error stops improving

Analysis of results:

- Calculate correlation coefficient (r) between predictions and actual values
- Verify model accuracy through regression analysis
- Compare predicted vs. actual values graphically

B. CASE 1

The NARX network utilized a default sigmoid transfer function in the hidden layer and a linear transfer function in the output layer. There were two inputs: an external input and a feedback input from the network's output. For training purposes, the network was configured with one hidden neuron and two delays, as illustrated in Figure 7. Where the Levenberg-Marquardt training algorithm was employed, indicating a robust optimization approach to minimize error. The performance metric used was the Mean Squared Error (MSE). The performance metric indicates a value of 881,

representing the prediction error. Three validation checks were conducted, ensuring that the process monitored performance to prevent overfitting. The NARX neural network was successfully trained over 15 iterations.

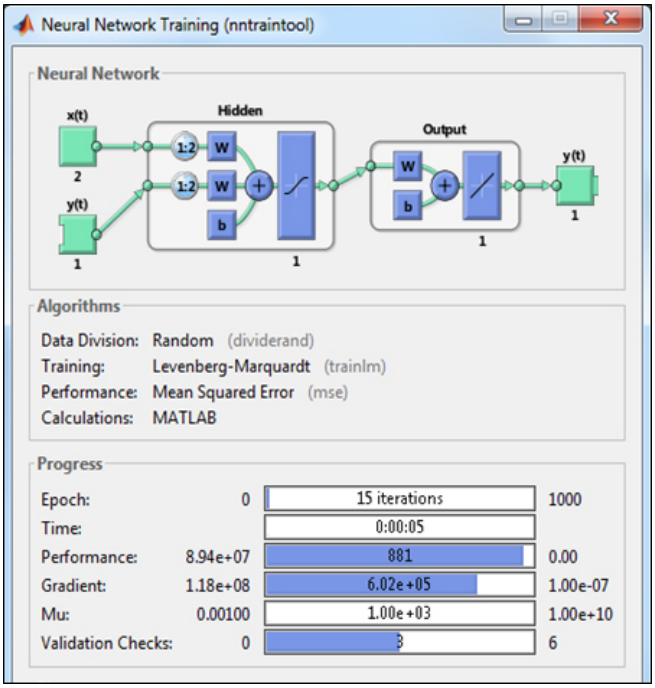

Fig. 7. NARX neural network training – Case 1

Figure 8 shows the performance of the NARX network, where the evolution of the Mean Squared Error (MSE) over 15 epochs is presented. The best validation performance was achieved at epoch 12, with an error of 99,665.90. The blue line represents the error on the training set, the green line corresponds to the validation error, and the red line denotes the test error. The training phase exhibited a progressive reduction in error, but from epoch 12 onwards, the validation and test errors began to increase, suggesting potential overfitting.

Figure 9 illustrates the correlation coefficients in the different phases where the regression analysis reveals that the predictions are well-aligned with the diagonal, indicating that the predicted values are highly consistent with the actual values. In the training phase, the correlation coefficient was R = 0.993, demonstrating a very strong relationship between the predicted and actual values. In the validation phase, R = 1, indicating a perfect fit. Similarly, in the test phase, R = 1, confirming a strong correlation with the test data. When considering all data points, the overall correlation coefficient was R = 0.991, reaffirming that the neural network exhibits excellent predictive performance. In all regression plots, the data points are closely aligned with the ideal regression line y = t, indicating high prediction accuracy. Regarding network fitting, the regression lines (dotted lines) are very close to the ideal line y = t, further supporting the precision of the predictions.

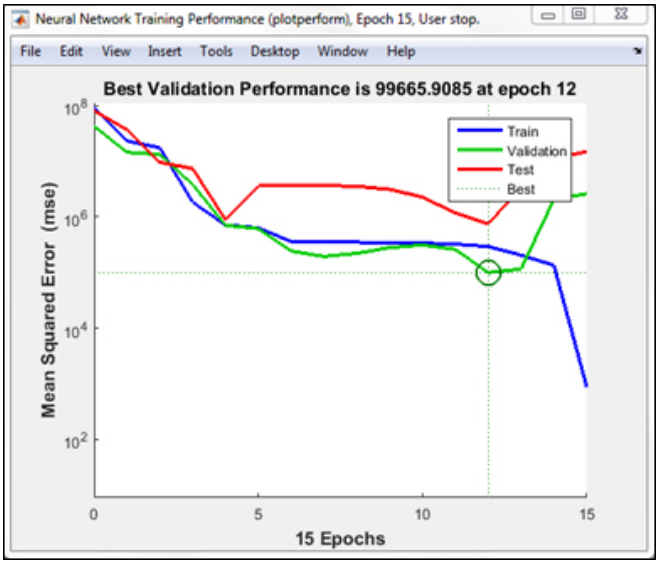

Fig. 8. NARX neural network performance – Case 1

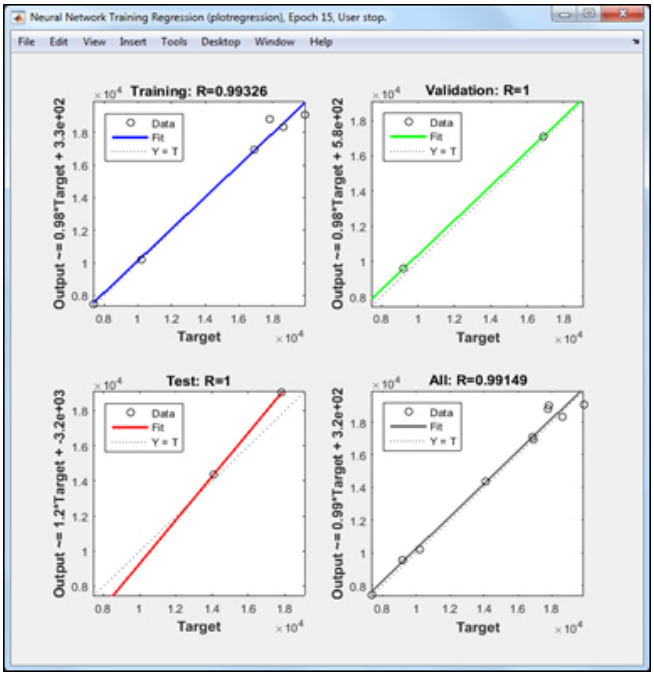

Fig. 9. Correlations of the NARX neural network – Case 1

C. CASE 2

The NARX network utilized a default sigmoid transfer function in the hidden layer and a linear transfer function in the output layer. There were two inputs: an external input and a feedback input from the network's output. For training purposes, the network was configured with one hidden neuron and one delay, as shown in Figure 10 where the Levenberg-Marquardt training algorithm was employed, indicating a robust optimization approach to minimize error. The performance metric used was the Mean Squared Error (MSE). A total of 27 iterations were completed out of a maximum

of 1000. The network training was successful, as the error significantly decreased and the gradient converged.

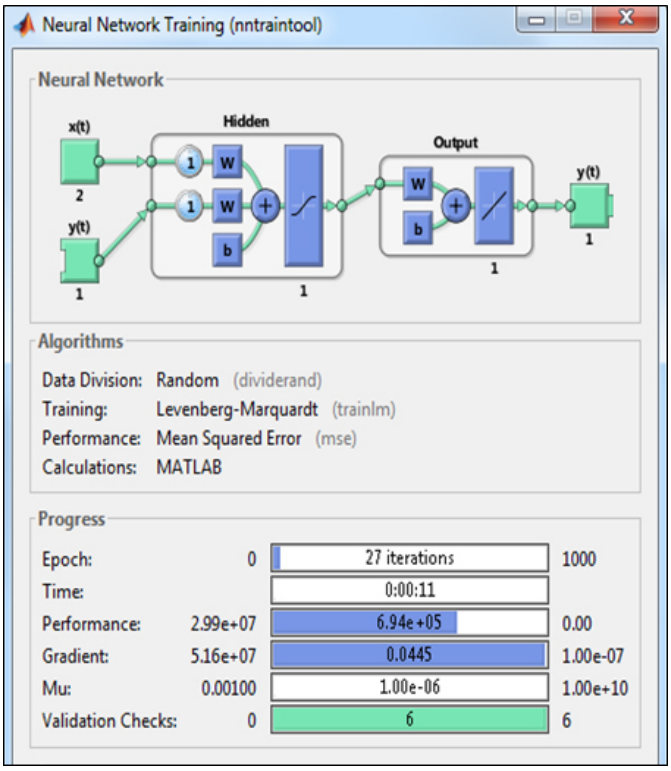

Fig. 10. NARX neural network training – Case 2

Figure 11 shows the performance of the NARX network where the evolution of the Mean Squared Error (MSE) during training is analyzed. The validation process stopped at epoch 21, when the MSE in validation ceased to improve. The red curve (test error) exhibits fluctuations, which may suggest the presence of noise in the data. The blue curve (training error) shows a continuous decrease. The best validation performance occurred at epoch 21, with an MSE of 1,867,351.20. The model was halted at an appropriate point to prevent overfitting. The validation results indicate that the model generalizes well.

Figure 12 illustrates the correlation coefficients in the different phases where the regression analysis reveals that the predictions align closely with the diagonal, indicating that the predicted values are highly consistent with the actual values. In the training phase, the correlation coefficient was R = 0.976 indicating a high correlation. In the validation phase, R = 1.0, signifying a perfect fit. In the test phase R = 0.967, demonstrating a strong correlation in test data. The overall correlation coefficient was R = 0.968, confirming that the neural network predicts with high accuracy. Regarding network fitting, the regression lines (dotted lines) are very close to the ideal y = t line, further supporting the precision of the predictions. The high R values in all phases confirm that the neural network maintains strong predictive performance.

The final results obtained are shown in the Table II where the average value of the correlation coefficients for the NARX

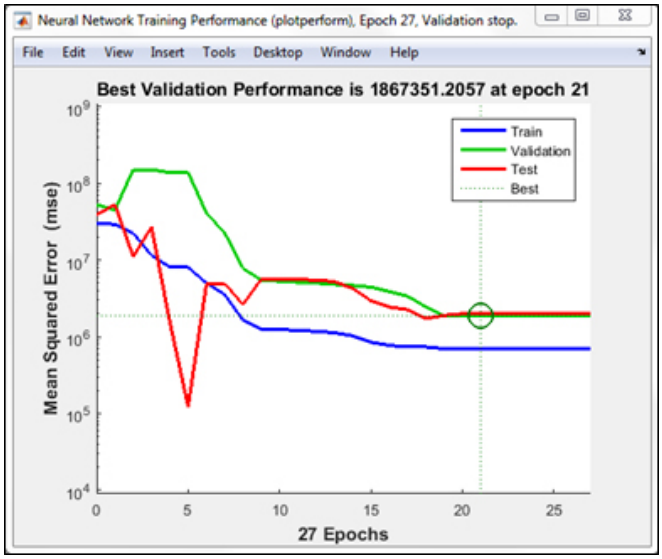

Fig. 11. NARX neural network performance – Case 2

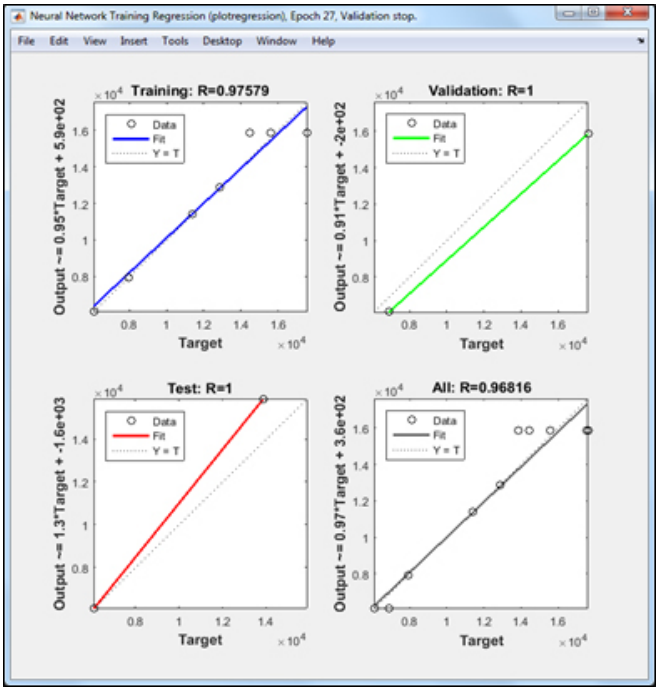

Fig. 12. Correlations of the NARX neural network – Case 2

model is 0.979.

Figure 13 presents the correlation coefficient r across three key phases (training, validation, and testing), as well as the overall correlation coefficient, for the two cases analyzed using the NARX neural network. In Case 1, the correlation coefficient is r = 0.993, indicating an excellent correlation between the predictions and actual values in the training phase. In contrast, Case 2 exhibits a slightly lower correlation coefficient of r = 0.976, suggesting that the model fit well but with a slight difference compared to the first case. Both cases demonstrate a perfect correlation (r = 1) in specific phases,

TABLE II
CORRELATION COEFFICIENTS - NARX MODEL

Neural network	Cases	Training phase - (r)	Validation phase - (r)	Test phase - (r)	Global correlation coefficient - (r)
NARX model	Case 1	0.993	1	1	0.991
	Case 2	0.976	1	1	0.968
				Average:	0.979

indicating that the model achieved absolute accuracy in these instances. The overall correlation coefficient for case 1 is r = 0.991, confirming highly accurate performance, whereas Case 2 yields r = 0.968, which, while still high, suggests slightly lower precision compared to Case 1. The global average of the correlation coefficients (0.979) indicates that, overall, the NARX network exhibits a high predictive capability for this problem.

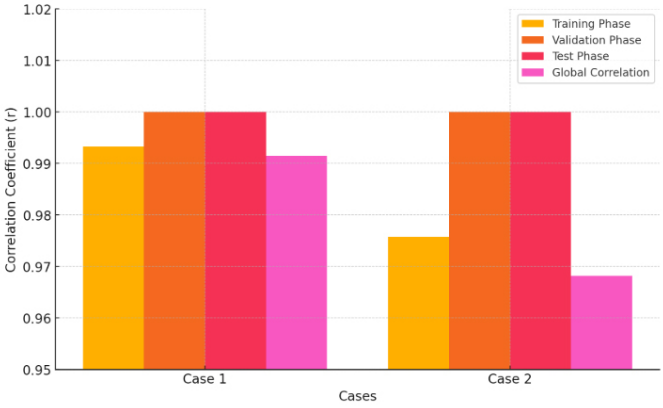

Fig. 13. Comparison of correlation coefficients in each phase

Figure 14 represents the magnitude of the correlation coefficients across each phase for both cases. Values closer to 1 are depicted in warm colors (red), while lower values appear in cool colors (blue). In both cases, the correlation values are extremely high across all phases, reinforcing the idea that the model has achieved a precise fit. In the training phase, Case 1 (r = 0.993) exhibits a better fit than Case 2 (r = 0.976), suggesting that the model in Case 1 has learned the training data patterns more effectively. The overall correlation in Case 2 (r = 0.968) is lower than in Case 1 (r = 0.991), indicating that the model in Case 2 may not generalize as well as the model in Case 1. The heatmap confirms the observations from the bar chart: the model demonstrates excellent accuracy.

Figure 15 illustrates the variation of the correlation coefficient r across the training, validation, and testing phases, as well as the overall correlation coefficient for both cases. It is observed that in the training phase, Case 1 exhibits a higher correlation coefficient (r = 0.993) compared to Case 2 (r = 0.976), indicating that the model in Case 1 has learned the training data patterns more effectively. The overall correlation

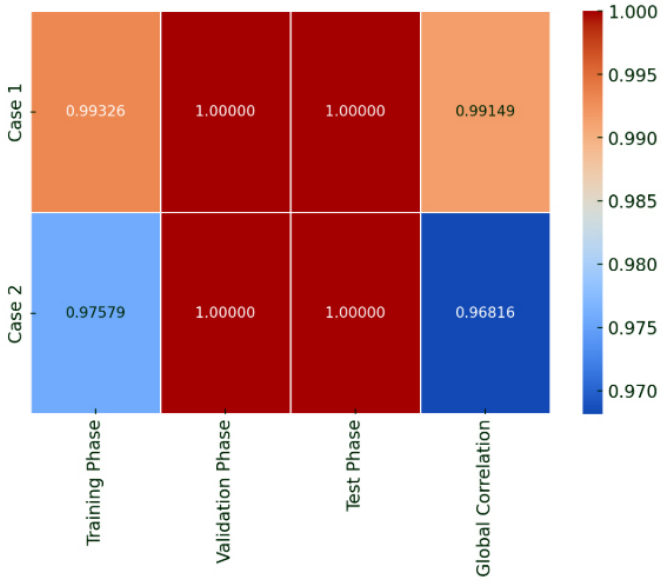

Fig. 14. Visualization of correlation strength

coefficient also demonstrates that Case 1 (r = 0.991) achieves a better overall fit than Case 2 (r = 0.968), reflecting superior general performance.

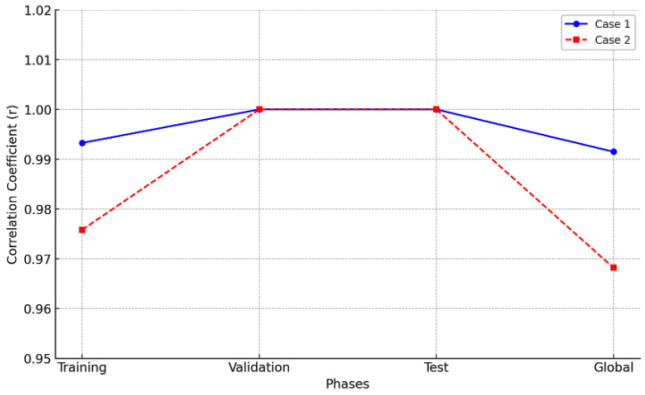

Fig. 15. Evolution of correlation coefficients across phases

Figure 16 compares the values predicted by the neural network with the actual values, where the black dashed line represents the ideal fit (y = x). In Case 1 (blue points), the predicted values are closely aligned with the ideal fit line, indicating high prediction accuracy. In Case 2 (red points), the predicted values exhibit slightly greater dispersion from the ideal line, suggesting that the model has slightly lower precision compared to Case 1. The plot confirms that Case 1 achieves better prediction accuracy for energy generation values. While Case 2 remains accurate, it shows greater dispersion compared to Case 1. This reinforces the conclusion that the model in Case 1 generalizes better than the one in Case 2.

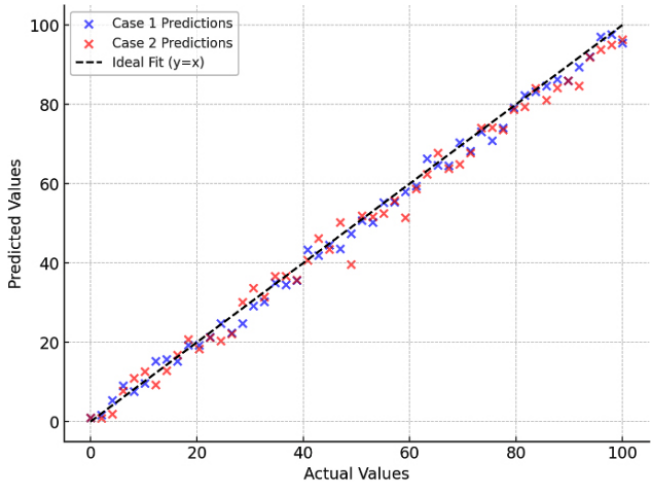

Fig. 16. Relationship between actual and predicted values

V. Conclusion

The NARX neural network has demonstrated exceptional effectiveness in predicting electrical energy generation from photovoltaic plants, achieving accuracy levels above 97% in the two analyzed cases, with correlation coefficients of 0.991 and 0.968, which shows that historical values of electrical generation and solar radiation constitute highly reliable predictors for future energy production. This predictive capability has important implications for the optimization and management of renewable energies, allowing for adjustment of operational parameters to maximize efficiency, significantly reducing operation and maintenance costs through more effective planning, facilitating the integration of solar energy into existing electrical grids by minimizing the need for backup energy sources, and improving the economic viability of photovoltaic projects, making them more competitive compared to conventional energy sources; these results suggest that predictive systems based on NARX networks represent an effective strategy to overcome the inherent variability of solar energy, with potential to extend to other renewable energy technologies in future research.

References

[1] M. Wei, M. Ye, J. B. Li, Q. Wang and X. Xu, "State of Charge Estimation of Lithium-Ion Batteries Using LSTM and NARX Neural Networks," in IEEE Access, vol. 8, pp. 189236-189245, 2020, doi: 10.1109/ACCESS.2020.3031340.

[2] Y. Xue, "Energy internet or comprehensive energy network?," in Journal of Modern Power Systems and Clean Energy, vol. 3, no. 3, pp. 297-301, September 2015, doi: 10.1007/s40565-015-0111-5.

[3] G. T. Heydt, R. Ayyanar, K. W. Hedman and V. Vittal, "Electric Power and Energy Engineering: The First Century," in Proceedings of the IEEE, vol. 100, no. Special Centennial Issue, pp. 1315-1328, 13 May 2012, doi: 10.1109/JPROC.2012.2187130.

[4] A. Blakers, M. Stocks, B. Lu, C. Cheng and R. Stocks, "Pathway to 100% Renewable Electricity," in IEEE Journal of Photovoltaics, vol. 9, no. 6, pp. 1828-1833, Nov. 2019, doi: 10.1109/JPHOTOV.2019.2938882.

[5] Global Off-Grid Lighting Association and Solar Energy Indsutry. (2020). Off-Grid Solar—Market Trends Reprot 2020. Accessed: Apr. 1, 2021. [Online]. Available: https://www.lightingglobal.org/wp-content/uploads/2020/03/VIVID

[6] L. Cozzi et al., "World energy outlook 2020," Int. Energy Agency, Paris, France, 2020.

[7] E. Bellini, "Solar retains it LCOE edge in latest lazard analysis," PV Mag., vol. 1, pp. 1–2, 2021.

[8] F. Uleman, V. Neder, A. Cordaro, A. Alù, and A. Polman, "Resonant metagratings for spectral and angular control of light for colored rooftop photovoltaics," ACS Appl. Energy Mater., vol. 3, pp. 3150–3156, 2020.

[9] R. A. Agathokleous and S. A. Kalogirou, "Status, barriers and perspectives of building integrated photovoltaic systems," Energy, vol. 191, 2020, Art. no. 116471.

[10] M. Heinrich et al., "Potential and challenges of vehicle integrated photovoltaics for passenger cars," in Proc. 37th Eur. PV Sol. Energy Conf. Exhib., 2020, pp. 1695–1700.

[11] S. Hubbard et al., "Nanostructured photovoltaics for space power," J. Nanophotonics, vol. 3, 2009, Art. no. 031880.

[12] A. W. Y. Ho-Baillie et al., "Deployment opportunities for space photovoltaics and the prospects for perovskite solar cells," Adv. Mater. Technol., vol. 7, 2022, Art. no. 2101059.

[13] S. W. Tabernig et al., "Avoiding Shading Losses in Concentrator Photovoltaics Using a Soft-Imprinted Cloaking Geometry," in IEEE Journal of Photovoltaics, vol. 12, no. 5, pp. 1116-1127, Sept. 2022, doi: 10.1109/JPHOTOV.2022.3182277.

[14] 100% Renewable Europe How to Make Europe's Energy System ClimateNeutral Before 2050, Solar Power Europe, Brussels, Belgium, 2020.

[15] S. Langer, "Analysis of the rate of convergence of fully connected deep neural network regression estimates with smooth activation function," J. Multivariate Anal., vol. 182, Mar. 2021, Art. no. 104695.

[16] N. Aljojo, A. Alshutayri, E. Aldhahri, S. Almandeel and A. Zainol, "A Nonlinear Autoregressive Exogenous (NARX) Neural Network Model for the Prediction of Timestamp Influence on Bitcoin Value," in IEEE Access, vol. 9, pp. 148611-148624, 2021, doi: 10.1109/ACCESS.2021.3124629.

[17] W. Wu, L. Li, J. Yin, W. Lyu and W. Zhang, "A Modular Tide Level Prediction Method Based on a NARX Neural Network," in IEEE Access, vol. 9, pp. 147416-147429, 2021, doi: 10.1109/ACCESS.2021.3124250.

[18] X. Qin, M. Gao, Z. He, and Y. Liu, "State of charge estimation for lithiumion batteries based on NARX neural network and UKF," in Proc. IEEE 17th Int. Conf. Ind. Informat. (INDIN), vol. 1. Finland: IEEE, Jul. 2019, pp. 1706–1711, doi: 10.1109/INDIN41052.2019.8972319.

[19] A. S. Ogundana, P. K. Terala, M. Y. Amarasinghe, X. Xiang and S. Y. Foo, "Electric Vehicle Battery State of Charge Estimation With an Ensemble Algorithm Using Central Difference Kalman Filter (CDKF) and Non-Linear Autoregressive With Exogenous Input (NARX)," in IEEE Access, vol. 12, pp. 33705-33719, 2024, doi: 10.1109/ACCESS.2024.3371883.

[20] MathWorks, "Design Time Series NARX Feedback Neural Networks". MathWorks.com. Available: https://www.mathworks.com/help/deeplearning/ug/design-time-series-narx-feedback-neural-networks.html. [Accessed: May. 2024].

[21] J. Liu, T. Li, Z. Zhang and J. Chen, "NARX Prediction-Based Parameters Online Tuning Method of Intelligent PID System," in IEEE Access, vol. 8, pp. 130922-130936, 2020, doi: 10.1109/ACCESS.2020.3007848.

[22] I. J. Leontaritis and S. A. Billings, "Input-output parametric models for non-linear systems Part I: Deterministic non-linear systems," Int. J. Control, vol. 41, no. 2, pp. 303–328, Feb. 1985, doi: 10.1080/0020718508961129.

[23] A. Andalib and F. Atry, "Multi-step ahead forecasts for electricity prices using NARX: A new approach, a critical analysis of one-step ahead forecasts," Energy Convers. Manage., vol. 50, no. 3, pp. 739–747, Mar. 2009, doi: 10.1016/j.enconman.2008.09.040.

[24] O. Fernández Zamudio, "Análisis de producción y rentabilidad de proyectos fotovoltaicos," Final Year Project, Industrial Engineering (Plan 98), Universidad de Sevilla, Seville, Spain, Apr. 2011.